Published in final edited form as:
Exp Eye Res. 2013 July ; 112: 57–67. doi:10.1016/j.exer.2013.04.006.

Formation of lipofuscin-like material in the RPE Cell by different components of rod outer segments

Lei Lei[a,b,1], **Radouil Tzekov**[b,1,2], **J. Hugh McDowell**[c], **Wesley C. Smith**[c], **Shibo Tang**[a], and **Shalesh Kaushal**[b,d,*]

[a]State Key Laboratory of Ophthalmology, Zhongshan Ophthalmic Center, Sun Yat-sen University, No. 54 South Xianlie Road, Guangzhou 510060, China

[b]The Department of Ophthalmology, University of Massachusetts Medical School, 381 Plantation Street, Worcester, MA 01605, USA

[c]The Department of Ophthalmology, University of Florida Health Science Center, 1600 SW Archer Road, Gainesville, FL 32610, USA

[d]Retina Specialty Institute, 6717 NW 11th Place, Gainesville, FL 32605, USA

Abstract

The mechanisms that control the natural rate of lipofuscin accumulation in the retinal pigment epithelial (RPE) cell and its stability over time are not well understood. Similarly, the contributions of retinoids, phospholipids and oxidation to the rate of accumulation of lipofuscin are uncertain. The experiments in this study were conducted to explore the individual contribution of rod outer segments (ROS) components to lipofuscin formation and its accumulation and stability over time. During the period of 14 days incubation of ROS, lipofuscin-like autofluorescence (LLAF) determined at two wavelengths (530 and 585 nm) by fluorescence-activated cell sorting (FACS) was measured from RPE cells. The autofluorescence increased in an exponential manner with a strong linear component between days 1 and 7. The magnitude of the increase was larger in cells incubated with 4-hydroxynonenal (HNE-ROS) compared with cells incubated with either bleached or unbleached ROS, but with a different spectral profile. A small (10–15%) decrease in LLAF was observed after stopping the ROS feeding for 14 days. The phagocytosis rate of HNE-ROS was higher than that of either bleached or unbleached ROS during the first 24 h of supplementation. Among the different ROS components, the increase of LLAF was highest in cells incubated with all-*trans*-retinal. Surprisingly, incubation with 11-*cis*-retinal and 9-*cis*-retinal also resulted in strong LLAF increase, comparable to the increase induced by all-*trans*-retinal. Supplementation with liposomes containing phosphatidylethanolamine (22: 6-PE) and phosphatidylcholine (18:1-PC) also increased LLAF, while incubation with opsin had little effect. Cells incubated with retinoids demonstrated strong dose-dependence in LLAF increase, and

*Corresponding author. Retina Specialty Institute, 6717 NW 11th Place, Suite C, Gainesville, FL 32605, USA. Tel.: +1 352 792 1193; fax: +1 352 484 1776. skaushal@retinaspecialty.com (S. Kaushal).
[1]The first two authors contributed equally to this work.
[2]Present address: The Roskamp Institute, 2040 Whitfield Ave., Sarasota, FL 34243, USA.

Contributions: S.K. and L.L. planned the experiments, L.L. did RPE cell culture, treatment and imaging, L.L. and R.T. did FACS and statistical analysis, H.M. did ROS isolation, R.T., L.L., W.S., S.T., and S.K. wrote the manuscript.

the magnitude of the increase was 2–3 times higher at 585 nm compared to 530 nm, while cells incubated with liposomes showed little dose-dependence and similar increase at both wavelengths. Very little difference in LLAF was noted between cells incubated with either unbleached or bleached ROS under any conditions. In summary, results from this study suggest that supplementation with various ROS components can lead to an increase in LLAF, although the autofluorescence generated by the different classes of components has distinct spectral profiles, where the autofluorescence induced by retinoids results in a spectral profile closest to the one observed from human lipofuscin. Future fluorescence characterization of LLAF in vitro would benefit from an analysis of multiple wavelengths to better match the spectral characteristics of lipofuscin in vivo.

Keywords

retinal pigment epithelium; lipofuscin; outer segment; lipid peroxidation; retinoids; autofluorescence; age-related macular degeneration

1. Introduction

Lipofuscin is a conglomerate of lipid-containing pigment granules representing partial lysosomal digestion and has been described in many somatic and neuronal cells, including the retinal pigment epithelium (RPE) (Jung et al., 2007; Sparrow et al., 2010a). RPE lipofuscin is the main source of retinal autofluorescence (AF) and its excessive levels eventually lead to cell death as part of the pathophysiological process in several sight-threatening diseases such as the dry form of age-related macular degeneration (ARMD) and Stargardt disease (Schmitz-Valckenberg et al., 2009).

The human outer retina is exposed to relatively high oxygen tension and intense light, two factors that result in high levels of lipid peroxidation in the biological membranes of photoreceptors and particularly in the rod outer segments (ROS). RPE lipofuscin content increases with age, and the topographical distribution of this process matches the distribution of rods in the retina (Weiter et al., 1986; Wing et al., 1978). Thus, in the macular region in humans, the area occupied by lipofuscin in an RPE cell increases from ~1% in the first decade of life to ~19% in the 9th decade of life (Feeney-Burns et al., 1984). A similar, approximately 20 fold increase in lipofuscin content as measured by fluorescence spectroscopy was observed also over the lifespan in mice (Mukherjee et al., 2009). The characteristics of this increase are somewhat uncertain as some studies showed a relatively rapid increase during the first 2 decades of life in humans, but a more moderate rate of increase in later decades (Feeney-Burns and Eldred, 1983; Feeney-Burns et al., 1984; Weiter et al., 1986). Recent studies employing mathematical and biophysical models of lipofuscin accumulation suggest that the increase is mostly linear over the human lifespan (Family et al., 2010; Mazzitello et al., 2009). On the other hand, there is insufficient information about the time course of lipofuscin or lipofuscin-like material accumulation in RPE cell culture and whether or not it is similar to the rate of accumulation in vivo.

Previous studies report that supplementation with ROS modified by lipid peroxidation contribute to the generation of lipofuscin granules in the RPE (Kaemmerer et al., 2007;

Krohne et al., 2010). However, the human retina is also exposed to different illumination conditions during daytime and night hours and it is unclear how this change in illumination could affect the increase in autofluorescence observed with modified ROS. The rate of ROS phagocytosis by the RPE and the efficiency of ROS intracellular degradation are key factors vital for the maintenance and normal functioning of the outer retina and are important factors in controlling the daily accumulation and clearance of RPE lipofuscin (Terman et al., 2007), yet it is not well understood if the accumulation of lipofuscin is related to different phagocytosis rate or to different intracellular degradation rate. Furthermore, it is uncertain to what extent lipofuscin material can be degraded by the RPE cells over time without any therapeutic intervention. A previous study by Boulton et al. (1989) suggests that this may not be the case, since they were not able to detect a change in the concentration of autofluorescent material if cultures supplemented with ROS for 2 months, which were then maintained an additional 2 months in culture medium without ROS supplementation. These observations were qualitative, and it remains likely that some degradation occurred, but its detection would require a proper quantitative assay.

Autofluorescence is an important characteristic of lipofuscin as it is one of the few observable and measurable parameters to be recorded during lifetime. The spectral profile of the bisretinoid A2E is one that matches closely the one the spectral profile recorded from lipofuscin granules (Sparrow and Boulton, 2005). Whether or not products of the lipid peroxidation of the outer segments also contribute to the AF from RPE cells detected in vitro or in vivo remains an open question. Additionally, the presence in the outer retina and the RPE of various retinoids and products of the retinoid visual cycle, leads to the possibility of formation of bisretinoids and their derivatives, which can affect the function of the lysosomes or be toxic to other cellular components. Both lipid peroxidation and retinoid/bisretinoid derivatives formation can contribute to the generation of non-degradable RPE material, or lipofuscin granules. However, the role of different components of the photoreceptor outer segments (phospholipids, retinoids, and proteins) in maintaining the overall RPE lipofuscin levels relatively low during the process of normal aging is unknown.

Another uncertainty related to using the RPE cell culture as model for lipofuscin accumulation in vivo is the spectral profile of the obtained autofluorescence. When quantifying RPE lipofuscin accumulation by fluorescence-activated cell sorting (FACS) appropriate emission filters and corresponding wavelengths need to be used. Nearly all studies in the past have used filters with single peak transmission wavelength of detection at 530 nm (Krohne et al., 2010; Rakoczy et al., 1992, 1994; Sugano et al., 2006). Although results obtained in this spectral region provide important information, quantitative autofluorescence may incompletely distinguish between fluorescent species like lipofuscin, ceroid, free lipid peroxidation products and other unspecified autofluorescence (Sheehy, 2002). Thus, it is important to look also at a longer wavelength spectral region (580–620 nm), which matches more closely the peak emissions from human lipofuscin in vitro and in vivo (Docchio et al., 1991; Haralampus-Grynaviski et al., 2003).

Our experiments were designed to address some of the outlined problems and uncertainties related to the use of RPE cell culture as a model for lipofuscin accumulation.

2. Materials and methods

2.1. ROS isolation

ROS isolation was performed according to a published method (McDowell, 1993). Retinas were dissected from adult cattle eyes under red light, which had been enucleated shortly after slaughter and placed in the dark on ice for a few hours before use. ROS were sometimes prepared immediately after dissection, but more often the retinas were frozen by dropping into liquid N_2 and stored at −80 °C until use. The ROS was immersed in a solution containing 0.1 M $NaPO_4$, 1 mM $MgC1_2$, 0.1 mM EDTA, pH 7.0 and contain 0.5 mM DTT. The retinas were vigorously shaken in 45% (w/v) sucrose. The ROS were first floated on 45% sucrose, then sedimented in 15% sucrose, and finally subjected to discontinuous sucrose density gradient centrifugation. Purified ROS were collected from the interface between layers of 0.77 M and 0.92 M sucrose. After diluting with buffer and pelleting, the ROS were suspended in buffer and stored frozen in small aliquots at −80 °C.

2.2. RPE cell culture, ROS modification and bleaching

2.2.1. RPE cell culture—ARPE-19 cells were cultured and maintained as described before (Lei et al., 2012; Strunnikova et al., 2001). Briefly, ARPE-19 cells were procured from the ATCC (Manassas, VA) and grown in high glucose DMEM (Cellgro/Mediatech Inc., Manassas, VA) supplemented with 10% heat-inactivated fetal calf serum FCS (Sigma–Aldrich, St. Louis, MO) and 1% penicillin/streptomycin (Gibco, Grand Island, NY) at 37 °C in presence of 5% CO_2. Cells were routinely subcultured or harvested for experiments using TrypLE Express (Gibco). For all subsequent experiments, cells were grown from the frozen aliquots to ensure that all experiments were conducted on similar cells between P2 to P8. ROS were prepared from cattle eyes following a described method (Papermaster, 1982). The yield was normally 10–20 nmol of rhodopsin per retina with an OD280/OD500 ratio of 2.3–2.6. Protein content of ROS preparations was measured by BioRad BC kit (Bio-Rad Laboratories, Hercules, CA).

2.2.2. ROS modification—Oxidized ROS using 4-hydroxynonenal (HNE) were prepared as described before (Kaemmerer et al., 2007). ROS were incubated with 5 mM HNE at room temperature overnight on a shaker. Unbound HNE was removed by repeated washes in PBS. The concentrations of protein modifications resulting from this procedure have been reported previously (Kaemmerer et al., 2007). Modified ROS were stored at −80 °C until use.

2.2.3. Bleaching—The native ROS were bleached under fluorescent white light conditions (700 lux) on ice (4 °C) for 1 h and then immediately applied to the RPE cells. Unbleached ROS were added in the dark under dim red light.

2.3. RPE cell treatment

Post confluent, stationary ARPE-19 cells (same passage) cultures in 10 cm plate were trypsinized, plated in 24 wells or 8-well chamber slide at a confluent density of $1.66*10^5/cm^2$.

2.3.1. Time-course experiments—After an additional culturing for 7 days, different types of ROS were added every day for 14 days. Periodically, on days 1, 3, 5, 7 and 14, samples were taken for FACS analysis. In another experiment, cells were incubated with different types of ROS for 7 days and then the incubation was stopped and FACS readings were taken on day 14 and day 21. The types of ROS were: unbleached ROS, bleached ROS and HNE-modified ROS (see above). Cells were always fed in the morning and the culture medium and the ROS were renewed daily. In pilot experiments, cells were incubated with ROS concentrations equivalent to 4 μg total ROS protein per cm^2 growth area, in a way similar to a published method (Krohne et al., 2010). FACS and fluorescence microscopy were then taken for the AF analysis.

2.3.2. Different component's contribution to AF—After an additional culturing for 7 days, several ROS components were added separately: 11-*cis* retinal, all-*trans* retinal, 9-*cis* retinal, opsin, liposome. All-*trans*-retinal (Sigma–Aldrich, St Louis, MI), 9-*cis*-retinal (Sigma–Aldrich) or 11-*cis*-retinal (National Eye Institute, Bethesda, MD) were all fed dissolved in ethanol at a concentration of 10 μM, except in the dose–response experiments, where the concentrations of 5 μM and 1 μM were also used. Liposomes were prepared as described below and fed at concentration of 5 μM, as pilot experiments demonstrated cell death at higher concentrations. Opsin was extracted from bleached ROS by removing endogenous retinoids using rho-1D4-coupled CNBr-activated sepharose beads as published previously (Noorwez et al., 2008) and was dissolved in PBS containing 1.0% dodecyl maltoside and 1 × protease inhibitor cocktail. It was fed in a concentration of 4 μg per cm^2 growth area.

2.4. ROS phagocytosis determination

2.4.1. Fluorescent labeling of ROS—The fluorescent labeling of ROS was done according to a published method (Lei et al., 2012). Briefly, isolated ROS were pelleted in 1× PBS, resuspended in serum-free culture medium (RPMI or MEM) and transferred to a 1.5-ml microcentrifuge tube for fluorescent staining. 2 mg/ml stock solution of FITC (Molecular Probes, Junction City, OR) in 0.1 mol/1 sodium bicarbonate, pH 9.0–9.5, was prepared under dim red light, filter-sterilized, and stored in aliquots at −20 °C. The FITC stock was added to the resuspended ROS (final concentration 10 μg/ml), and incubation was continued for 1 h at room temperature in the dark. The FITC-stained ROS (FITC-ROS) were pelleted in a microcentrifuge (4 min at 7000 rpm) and resuspended in growth medium.

2.4.2. Incubation of cultured RPE cells with FITC-ROS—For FACS, post confluent, ARPE cells were fed with FITC-labeled ROS at 4ug/cm^2 similar to the method described before (McLaren et al., 1993) and incubated at 37 °C for periods of 1 h–24 h. At the end of the incubation time, unattached FITC-ROS were removed and the cells were washed three times with cold HBSS. To quench external bound ROS and assure purity, samples were incubated with 0.4% trypan blue for 10 min. These measures to enhance ROS purity were similar to the ones described in the literature (McLaren et al., 1993; Miceli and Newsome, 1994). FACS analysis was performed at the end of incubation time.

For confocal microscopy, the ARPE cells were stained with LysoTracker Red DND-99 (Molecular Probes, Junction City, OR) at 75 nM for 2 h after the incubation with FITC-ROS.

2.5. Liposome preparation

22:6 phosphatidylethanolamine (22:6 PE) and 18:1 (Δ9-Cis) phosphatidylcholine (18:1 PC, Avanti Polar Lipids Inc, Alabaster, AL) were mixed at a ratio of 6:4 to a final concentration of 10 mM. The solvent was dried out by argon at room temperature and PBS 1× was added. Liposomes were extruded with Avanti® Mini-Extruder (Avanti Polar Lipids Inc., Alabaster, AL) to extrude liposomes with an average diameter of 100 nm. Extruded vesicles were stored at 4 °C for 3–4 days.

2.6. Flow cytometry

Cells were cultured in 24-well plates and incubated with different components as described previously. Cells were repeatedly washed, detached with trypsin, and analyzed on C6 flow cytometer (Accuri Cytometers, Inc. Ann Arbor, MI). A gate was set to exclude cell debris and cell clusters, and 10,000 gated events were recorded. Experiments were performed in triplicates. Two channels were used with excitation wavelength of 488 nm: FITC/GFP channel (533/30 nm) and the PE/PI channel (585/40 nm). The autofluorescence ratio was defined as published (Lei et al., 2012), namely as a ratio between the fluorescence detected by the test groups (treated with ROS or with ROS components) vs. the control group (no treatment).

2.7. Fluorescence microscopy/confocal microscopy

Cells were cultured in 8-well microscopy glass slides (Lab-Tek Chamber Slide; Nunc, Langenselbold, Germany) and treated with different components as described. After 7 days feeding, cells were repeatedly washed to remove non-internalized ROS, fixed with 4% paraformaldehyde (PFA), stained with 1 mg/ml DAPI (AppliChem, Darmstadt, Germany), and mounted in Vectashield mounting medium (Vector Laboratories, Burlingame, CA). Intracellular lipofuscin granules were documented on a Leica DM 6000 fluorescence microscope (Leica Microsystems, Wetzlar, Germany) using a fluorescein filter set with excitation at 480/40 nm and emission at 535/50 nm. Confocal microscopy was performed with Leica TCS SP5 Spectral point scanning confocal microscope with a Leica DMI 6000 CFS (Confocal Fixed Stage). Cells were labeled with 1 μg/ml Hoechst stain (Sigma–Aldrich) for 5–7 min and the 405 nm laser, the 488 nm and the 561 nm lasers were used at different aims. At UMass Medical School Digital Light Microscopy Core confocal microscopy was performed with a Solamere Technology Group (Salt Lake City, UT) CSU10B Spinning Disk Confocal System which consisted of a CSU10B spinning disk confocal scan head (Yokogawa Electric Corporation, Tokyo, Japan) with high efficiency dichroic mirrors and laser blocking filters attached to a Nikon TE2000-E2 motorized inverted fluorescence microscope equipped with Nikon's Perfect Focus System (PFS) (Nikon Instruments, Melville, NY) and a custom acousto-optical tunable filter (AOTF) controlled laser launch with 405 nm, 488 nm, 561 nm and 636 nm lasers.

2.8. Transmission electron microscopy

Transmission electron microscopy was carried as described in detail before (Lei et al., 2012). Briefly, Cells were fixed by adding 1 ml of 2.5% glutaraldehyde (v/v) in 0.75 M Na phosphate buffer (pH 7.2) to each of the wells in the culture plate and allowed to fix overnight at 4 °C. The next day the fixed samples were washed three times in 0.75 M Na phosphate buffer (pH 7.2). The cells were then scraped, pelleted, rinsed in DH_2O and post-fixed in 1% osmium tetroxide (w/v) in DH_2O. The fixed cells were then washed again in the DH_2O and dehydrated through a graded ethanol series. Samples were then infiltrated with epoxy resin, polymerized, trimmed and ultrathin sections were cut. The sections were then collected and mounted on copper support grids and were examined on a FEI Tecani 12 BT (FEI Inc., Hillsboro, OR) transmission electron microscope. Images were captured using a Gatan TEM CCD camera (Gatan Inc., Pleasanton, CA).

2.9. Statistical analysis

Differences in autofluorescence between the groups were tested with one-sample *t*-test, where the levels of autofluorescence from the control group were assigned to a value of 1. The threshold for significance (p) was set to <0.05. Values for $p > 0.01$ and $p < 0.05$ were considered significant and indicated with single asterisk *, values for $p > 0.001$ and $p < 0.01$ were considered very significant and indicted with double asterisk **. Both the statistical analysis and the curve fitting (as linear or non-linear regression) were conducted with GraphPad Prism v.5.0 software (GraphPad Software, Inc., La Jolla, CA).

3. Results

3.1. Lipofuscin accumulation in the RPE during the course of supplementation with different types of ROS

When ROS are modified with *4-hydroxynonenal* (HNE) and fed to ARPE cells, this results in an increase in LLAF at 530 nm (Krohne et al., 2010). Still, the time course of this effect, the spectral profile of the resulting autofluorescence at different wavelengths and whether or not bleaching of ROS would result in a similar increase in LLAF, are all unresolved questions. To systematically explore these issues, we incubated RPE cells with either unbleached, bleached or HNE-modified ROS for 14 days. FACS analysis was undertaken on days 1, 3, 5, 7 and 14. The result was an increase in LLAF over time at both wavelengths (530 nm and 585 nm) under all conditions tested (Fig. 1). However, the magnitude and the pattern of the increase were different for unmodified vs. HNE-modified ROS. Thus, when RPE cells were incubated with unmodified ROS, the relative increase in AF ratio was always higher at 585 nm compared to the increase observed at 530 nm, whereas the increase was practically the same for both wavelengths when cells were incubated with HNE-modified ROS (Fig. 1B–D). Under all these conditions, the time course of this increase could be well-described with a single exponential function, but exhibited also a well-defined linear component during the time period between Day 1 and Day 7 (Fig. 1B,C). During the period from day 7 to day 14, for five out of the six conditions tested (with the exception of bleached ROS and LLAF measured at 585 nm), the increase continued with a diminished rate, although no saturation was observed. Surprisingly, under the conditions of supplementation with bleached ROS and LLAF detected at 585 nm, the increase continued

in a linear manner with the same slope as during the previous period (Fig. 1C). Overall, the relative increase in LLAF as a result of supplementation with HNE-modified ROS was much higher compared to the increased observed after incubation with either bleached or unbleached ROS, especially during the first 7 days. Of note, LLAF levels were relatively stable in cells with only ~10–15% reduction over 2 weeks after ROS feeding was stopped, suggesting that some minimal degradation of lipofuscin-like material takes place even during this relatively short time period (Fig. 1B,C).

3.2. Relationship between rate of phagocytosis of ROS and LLAF increase

To deconvolute whether the observed increase in LLAF over time, especially from cell supplemented with oxidatively-modified ROS, is the consequence of enhanced phagocytosis or decreased degradation, we assessed the early kinetics (up to 24 h) of LLAF accumulation. The rate of LLAF increase was mirrored by a similar increase in the rate of phagocytosis (Fig. 2B), i.e. the oxidized ROS were phagocytized more rapidly than either the bleached or unbleached ROS. FITC-labeled ROS material co-localized with the fluorescent acidotropic probe Lysotracker, placing it in the lysosome, the cellular compartment where lipofuscin has been previously identified (Fig. 2A).

Furthermore, to confirm that ROS are phagocytized and undigested material can be present in the cell, a transmission electron microscopy was carried out. The typical appearance of intracellular perinuclear cytoplasmic inclusion bodies, containing a membranous swirl and phagolysosomes (round spots of electron-dense material) were observed (Fig. 3). These findings were similar to the ones observed in Figs. 4, 5 and 6 in Lei et al. (2012).

3.3. Contribution of individual ROS components to LLAF

Native ROS contains several major components, including retinoids (all-*trans*-retinal, 11-*cis*-retinal), proteins (predominantly opsin) and phospholipids including phosphatydilethanolamine (PE) and phosphatydilcholine (PC). Previous work has focused mostly on the in vitro formation of fluorophores from oxidized lipid–protein complexes or combinations of PE and all-*trans*-retinal (Boulton et al., 1989; Katz et al., 1996). Consequently, it is unclear what is the relative contribution of phospholipids or retinoids to LLAF. It is also undetermined whether or not bleaching of ROS could have an effect on LLAF. Therefore, we added bleached, unbleached ROS and several individual ROS components separately to RPE cells and examined the ensuing change in LLAF. Addition of either bleached or unbleached ROS resulted in a statistically significant, although very mild increase in LLAF at both wavelengths (Fig. 4A,B vs. Fig. 1C,D).

Addition of retinoids increased LLAF in a characteristic way, with a much larger increase observed at 585 nm, the typical emission maximum for human lipofuscin (Fig. 4) (Delori et al., 2011; Docchio et al., 1991; Haralampus-Grynaviski et al., 2003). The most prominent increase was detected from incubation of the RPE cells with all-*trans*-retinal, an increase that was ~20% higher when compared to the increase from addition of either 11-*cis* or 9-*cis*-retinal at 585 nm. The LLAF increase was approximately the same for cells fed with either of the three retinoids at 530 nm, the emission wavelength region most often reported in the

literature (Kennedy et al., 1996; Krohne et al., 2010; Rakoczy et al., 1992; Sugano et al., 2006).

Since the phospholipid content of ROS is high, we also fed the RPE cells with liposomes that were predominantly composed of 22: 6-PE (DHA-PE), the most abundant phospholipid in the outer segment (Fliesler and Anderson, 1983), but lacked retinoids or opsin. This led to a substantial increase in LLAF of approximately the same magnitude at 530 and 580 nm (Fig. 4A,B). Finally, addition of opsin alone resulted in a statistically significant ($p = 0.047$), but relatively small increase in LLAF, at 530 nm (27% increase) and no statistically significant changeat 585 nm (Fig. 4A,B).

3.4. Dose-dependence of the LLAF increase

In a separate experiment, it was explored whether or not a dose–dependence relationship exists between the amount of supplemented components and the detected change in LLAF. Supplementation of the cells with increasing amounts of any of the three retinoids resulted in a strong increase in LLAF in a clear dose-dependent manner. In contrast, addition of increasing concentrations of liposomes, resulted in a moderate increase and saturation at ~5 μM (Fig. 5A,B).

In a more limited way, a dose–dependence relationship was explored also for the effect of increasing the amount of supplementation with HNE-modified ROS. Thus, when cells were fed with HNE-modified ROS where the amount of oxidation was varied by 50%, the decrease in ROS oxidation resulted in a decrease in LLAF by ~25%. This change was not influenced by bleaching the ROS (Fig. 5C,D).

4. Discussion

In the present work, the time dependence of LLAF change as a result of incubation with three different types of ROS was tested for up to 14 days. When cells were incubated with unmodified ROS (either bleached or unbleached) a moderate increase in LLAF was observed. The rate of LLAF increase at 530 nm was comparable to the change observed by Rakoczy et al. (1992) from challenging a primary RPE cell culture from a 7-year old and a 47-yard old donors. Although the authors did not report the relative increase in autofluorescence of cells challenged with ROS vs. cells not challenged with ROS (as an AF ratio, like the one presented in the current report), from the data presented in their Fig. 3 it can be estimated that the increase in AF ratio from Day 1 to Day 7 occurred at a higher rate compared to the increase in LLAF observed later, similar to our observation, However, in addition to the observations at 530 nm showing similar change in LLAF to the one observed before, we made also observations at 585 nm, which showed slightly different dynamics.

The rate of increase in LLAF at 585 nm for cells incubated with bleached ROS was almost the same throughout the entire period of observation (14 days), while in the other two conditions the rate of increase diminished after 7 days. This is a novel observation which points to a different capacity of the RPE cell to handle phagocytosis of bleached vs. unbleached photoreceptor outer segments. One possible explanation is that this difference is related to the presence of larger quantities of all-*trans*-retinal in the bleached ROS and a

resulting slightly larger accumulation of undegradable products in the RPE cell, such as A2E (Sparrow et al., 1999). The well-characterized bisretinoid A2-E could impede the lysosomal function (Finnemann et al., 2002), or could inhibit directly the RPE65 enzyme and, thus, the whole retinoid visual cycle (Moiseyev et al., 2010). On the other hand, recent studies have shown that eyecup fluorescence in mice was independent of either dark or cyclic light rearing of the mice (Boyer et al., 2012). However, the later work also demonstrated that A2E accumulation was slightly higher in 129/sv and abca4−/− mice after the age of 3 months and until 12 months of age (their Fig. 4a,b), which is consistent with our observation and points to a more complex dynamics between A2E accumulation and autofluorescence than previously expected.

Supplementation with HNE-modified ROS led to a prominent increase in LLAF and this matches well with the previously published data by Krohne et al. (2010) detected at 530 nm for up to 7 days.

Furthermore, the linear rate of phagocytosis observed in the current study for unmodified ROS over the course of 24 h is in line with previous reports (Kennedy et al., 1996; McLaren et al., 1993). The relative increase in LLAF correlates very well with the greater initial rates of phagocytosis of HNE-ROS compared to the other two forms of ROS (Fig. 1B,C, Fig. 2B). The observation that HNE-modified ROS are phagocytosed at a higher rate compared to either unbleached or bleached ROS is a novel one, but is in line with similar findings by Sun et al. (2006), demonstrating that oxidation of ROS phospholipids may serve as physiological triggering signal for RPE phagocytosis mediated by CD36 and other surface receptors. This finding also suggests that the rate of phagocytosis is likely an important factor influencing the rate of early accumulation of lipofuscin-like material in the RPE cell. We have made similar observations recently when studying the effect of HNE-modified ROS on the phagocytosis and autofluorescence of microglial cells and macrophages (Lei et al., 2012). Thus, the similarity between RPE and other phagocytizing cells in the body in terms of LLAF time course and close relationship to the rate of phagocytosis points to a universal mechanism and possibly limitations to the capacity of phagocytizing cells to process extracellular material.

Although the best fit describing the increase in LLAF over time can be obtained with a single exponential model, the strong linear component observed between days 1 and 7 matches well with recent biophysical models of lipofuscin accumulation in humans (Family et al., 2010; Mazzitello et al., 2009) and also with the relatively monotonic increase in lipofuscin content observed between the second and sixth decade of life in human RPE (Feeney-Burns et al., 1984).

Another interesting aspect of the fate of lipofuscin-like material in the RPE cells is the possibility for a spontaneous degradation of already accumulated material inside the cells. Can lipofuscin be degraded once accumulated? Fenney-Burns et al. (1988) had inconclusive results in their study, while Boulton et al. (1989) did not observe lipofuscin degradation in cell culture. However, other in vivo studies (summarized by Katz (2002)), suggest otherwise. Furthermore, a reported decrease in A2-E administered to cultured human RPE cells (Schutt et al., 2007) and a recent report that a pharmacological intervention can

decrease the RPE lipofuscin content in monkeys (Julien and Schraermeyer, 2012), also points in that direction. Our observation of a limited decrease in LLAF after stopping the treatment is, to the best of our knowledge, the first direct quantitative observation of this phenomenon.

Mammalian photoreceptor outer segments are composed of phospholipids, proteins (mostly opsin) and retinoids (Fliesler and Anderson, 1983). We have sought to determine the relative contribution of each of these components to the formation of RPE lipofuscin-like material. It has been well-established that the lipid content of lipofuscin increases with age (Bazan et al., 1990; Feeney-Burns et al., 1988). Thus, it is likely that the inability of RPE cell lysosomal machinery to degrade lipids and phospholipids would be one of the main sources of lipofuscin accumulation in the RPE. Our results support such a mechanism and demonstrate that liposomes composed by 22:6-PE and 18:1-PC (in 6:4 ratio) contributes to LLAF. However, the spectral signature of this contribution is different when compared to the spectral signature of the contribution of other ROS components, like retinoids. Thus, LLAF generated by supplementation of liposomes increases in a similar way at both wavelengths measured (530 & 585 nm), while the LLAF resulting from supplementation of retinoids increases predominantly at 585 nm. Given the fact that the dominant emission wavelength range of human retinal lipofuscin determined in vitro or in vivo is in the region 580–620 nm (Delori et al., 2011, 1995; Docchio et al., 1991; Haralampus-Grynaviski et al., 2003) and that 8 out of the 10 fluorophores in chloroform extracts of RPE lipofuscin have emission peaks between 568 and 670 nm (Kennedy et al., 1995), it is reasonable to assume that phospholipids have a secondary contribution to LLAF. At this time, it is unclear whether other phospholipids, like phosphatidylserine, or cholesterol (which is ~10% of the lipid in the ROS membranes (Fliesler and Bretillon, 2010)), can also increase LLAF.

We also studied the effect of various retinoids on accumulation of lipofuscin. Addition of all-*trans*-retinal as well as 9-*cis* or 11-*cis* retinal to the RPE cells resulted in a several-fold increase in LLAF at 585 nm. Under physiological conditions, all-*trans*-retinal most likely interacts with PE in the ROS membrane to produce the bisretinoid A2E and its isomers, all fluorescent components of lipofuscin (Ben-Shabat et al., 2002; Wang et al., 1999). In our experimental setting, free all-*trans*-retinal could similarly interact with PE, which is abundantly present in the RPE cell membrane (Gulcan et al., 1993). Surprisingly, addition of 11-*cis*-retinal also induced LLAF at levels comparable to those induced by addition of all-*trans*-retinal. There are two possible explanations for this effect. First, it is possible that a fraction of 11-*cis*-retinal applied to the RPE cells isomerizes spontaneously to the all-*trans* form (Futterman and Futterman, 1974) upon interaction with the RPE cell membrane, thus facilitating the formation of A2E and other autofluorescent bisretinoids. However, this fraction should be relatively small and cannot explain the level of autofluorescence observed. More likely, application of 11-*cis*-retinal by itself could lead to generation of A2E and other related bisretinoids. This second possibility is strongly supported by recent findings that lipofuscin-like fluorophores in rod outer segments originate from 11-cis retinal (Boyer et al., 2012). The third retinoid tested in our experiments was 9-*cis*-retinal. Although not considered to be present in substantial quantities in human retina, it was demonstrated that it concentration can increase in the retina of some RPE65 knockout mice (Fan et al.,

2006). Additionally, it was shown that it could interact with PE of the RPE membrane in the dark (Groenendijk et al., 1980) and, thus, form an adduct that may contribute to LLAF as well. This is consistent with our observation of comparable effectiveness between 9-cis and 11-cis-retinal in terms of LLAF generation at both wavelengths studied (530 and 585 nm).

Bleaching of ROS had a rather small effect on magnitude of LLAF increase up to 7 days, both when applied to unmodified ROS or to HNE-modified ROS (Figs.1C,D, 3A,B and 4C,D). This was somewhat of an unexpected finding, as it is largely believed that all-*trans*-retinal is the primary source of bisretinoids in the retina, which are considered the main contributories to LLAF (Sparrow and Boulton, 2005; Sparrow et al., 2010a). This observation, together with the finding that both all-*trans*-retinal and 11-*cis*-retinal had similar effects on LLAF increase (Figs. 4A,B and 5A,B), suggests that both forms of retinal could contribute to LLAF increase and, therefore, to lipofuscin accumulation. This is supported by earlier work indicating that fluorescence intensity from RPE samples from rats maintained under dim cyclic light was higher compared to rats housed under bright cyclic light (Katz and Eldred, 1989). Furthermore, our observation is consistent with a recent work in transgenic mice and isolated photoreceptors indicating that both eyecup fluorescence and the rate of A2E accumulation over time is very similar for mice raised under darkness or cyclic light (Boyer et al., 2012).

Oxidized protein seems to be the dominating component (up to 58%) of extracocular lipofuscin (Jung et al., 2007). Analytical studies of retinal/RPE lipofuscin yielded contradictory results in published works. Bazan et al. (1990) and Warburton et al. (2005) found both proteins and lipids in lipofuscin. However, Feeney-Burns et al. (1988) and Schutt et al. (2002) were not able to detect opsin in lipofuscin granules, while Ng et al. (2008) concluded that human lipofuscin contains mostly retinoids and lipids and only minimal amounts of protein. Theoretically, protein degradation could be incomplete and could lead to generation of protein fragments, which may be misfolded and disturb the normal functioning of the RPE cell (Lin and Lavail, 2010; Tzekov et al., 2011). However, our data demonstrate very little relative contribution of opsin alone to the LLAF, and thus, argue against a significant contribution of opsin to lipofuscin formation.

Some limitations have to be considered when evaluating the results from the present study. Whilst the finding that LLAF increases overtime and the rate of increase seems to slow down after 7 days is very clear and supported by previous research, the duration of the experiments did not allow us to reach a point where LLAF would saturate. Hence, future longer-term experiments would provide a better answer to question of when the RPE cell would reach its capacity to handle lipofuscin-like material accumulation. Another aspect to keep in mind is that the ARPE-19 cells are non-melanotic, and, therefore, do not fully reflect the complex biogenesis of RPE lipofuscin in humans involving melanin and formation of melanolipofuscin. Furthermore, ARPE-19 cells have shown many similarities with the native RPE, and are likely to be one of the most widely used cells in retinal and RPE research, but they may differ in important ways from the native tissue, like alterations in gene profile, lack of apical processes, relatively low membrane resistance, etc. (Maminishkis et al., 2006). Although these differences are not critical, to fully understand the dynamics of

lipofuscin accumulation and clearance in humans, a comparison between ARPE-19 and other, primary, melanin-containing RPE cell cultures is warranted.

It is also possible that some non-specific uptake (in contrast to a purely receptor-mediated phagocytosis) may have been present, under current conditions, although, as pointed out in Materials and Methods, measures were taken to assure purity of ROS and to minimize the non-specific uptake.

In addition, although retinoids per se exhibit little if any autofluorescence when irradiated at 488 nm (Sparrow et al., 2010b) spontaneous autofluorescence of ROS, especially when oxidized cannot be excluded and could have contributed to the fluorescence detected in the present study.

Finally, as the lipofuscin and lipofuscin-like material fluorescence is complex and depends on the excitation wavelength and has a non-linear wavelength emission profile, it would be advantageous and is part of our future plans to conduct a more comprehensive evaluation with recording LLAF at more excitation and emission wavelengths.

5. Conclusions

Accumulation of lipofuscin-like material in the RPE cells exhibited a strong linear component between days 1 and 7, and bears some similarity to the expected rate of age-related lipofuscin accumulation in humans. Further, longer-term studies, could explore a possible correlation with the human RPE lipofuscin content in a more definitive manner. In such studies, it would be very desirable to record LLAF at longer wavelengths (including 585 nm), as the increase in LLAF intensity with time at this wavelength could differ substantially from the intensity observed at shorter wavelengths (including 530 nm). Our observations confirmed the importance of different retinoids, including 11-*cis*-retinal, in generating lipofuscin-like material in the RPE cell, but also suggest a sizeable contribution from phospholipids, while questioning any substantial role for opsin in this process.

Acknowledgments

We thank Paul Furcinitti of the University of Massachusetts Medical School Digital Light Microscopy Core Facility for help with confocal microscopy and live cell imaging. We thank Michael Brehm for help with FACS analysis, and Amit Roy for help with preparing the RPE cells. We thank Greg Hendrix for help with transmission electron microscopy. This work is supported by University of Massachusetts Department of Ophthalmology Research and Education fund. Preliminary reports of these findings were presented at the Annual Meeting of the Association for Research in Vision and Ophthalmology in Ft. Lauderdale, 2012.

References

Bazan HE, Bazan NG, Feeney-Burns L, Berman ER. Lipids in human lipofuscin-enriched subcellular fractions of two age populations. Comparison with rod outer segments and neural retina. Investigative Ophthalmology & Visual Science. 1990; 31:1433–1443. [PubMed: 2387677]

Ben-Shabat S, Parish CA, Vollmer HR, Itagaki Y, Fishkin N, Nakanishi K, Sparrow JR. Biosynthetic studies of A2E, a major fluorophore of retinal pigment epithelial lipofuscin. The Journal of Biological Chemistry. 2002; 277:7183–7190. [PubMed: 11756445]

Boulton M, McKechnie NM, Breda J, Bayly M, Marshall J. The formation of autofluorescent granules in cultured human RPE. Investigative Ophthalmology & Visual Science. 1989; 30:82–89. [PubMed: 2912915]

Boyer NP, Higbee D, Currin MB, Blakeley LR, Chen C, Ablonczy Z, Crouch RK, Koutalos Y. Lipofuscin and N-retinylidene-N-retinylethanolamine (A2E) accumulate in the retinal pigment epithelium in the absence of light exposure: their origin is 11-C is retinal. The Journal of Biological Chemistry. 2012

Delori F, Greenberg JP, Woods RL, Fischer J, Duncker T, Sparrow J, Smith RT. Quantitative measurements of autofluorescence with the scanning laser ophthalmoscope. Investigative Ophthalmology & Visual Science. 2011; 52:9379–9390. [PubMed: 22016060]

Delori FC, Dorey CK, Staurenghi G, Arend O, Goger DG, Weiter JJ. In vivo fluorescence of the ocular fundus exhibits retinal pigment epithelium lipofuscin characteristics. Investigative Ophthalmology & Visual Science. 1995; 36:718–729. [PubMed: 7890502]

Docchio F, Boulton M, Cubeddu R, Ramponi R, Barker PD. Age-related changes in the fluorescence of melanin and lipofuscin granules of the retinal pigment epithelium: a time-resolved fluorescence spectroscopy study. Photochemistry and Photobiology. 1991; 54:247–253. [PubMed: 1780361]

Family F, Mazzitello KI, Arizmendi CM, Grossniklaus HE. Statistical physics of age related macular degeneration. Physics Procedia. 2010; 4:21–33.

Fan J, Wu BX, Sarna T, Rohrer B, Redmond TM, Crouch RK. 9-cis Retinal increased in retina of RPE65 knockout mice with decrease in coat pigmentation. Photochemistry and Photobiology. 2006; 82:1461–1467. [PubMed: 16553465]

Feeney-Burns L, Eldred GE. The fate of the phagosome: conversion to ‘age pigment’ and impact in human retinal pigment epithelium. Transactions of the Ophthalmological Societies of the United Kingdom. 1983; 103 (Pt 4):416–421. [PubMed: 6589859]

Feeney-Burns L, Gao CL, Berman ER. The fate of immunoreactive opsin following phagocytosis by pigment epithelium in human and monkey retinas. Investigative Ophthalmology & Visual Science. 1988; 29:708–719. [PubMed: 2966778]

Feeney-Burns L, Hilderbrand ES, Eldridge S. Aging human RPE: morphometric analysis of macular, equatorial, and peripheral cells. Investigative Ophthalmology & Visual Science. 1984; 25:195–200. [PubMed: 6698741]

Finnemann SC, Leung LW, Rodriguez-Boulan E. The lipofuscin component A2E selectively inhibits phagolysosomal degradation of photoreceptor phospholipid by the retinal pigment epithelium. Proceedings of the National Academy of Sciences of the United States of America. 2002; 99:3842–3847. [PubMed: 11904436]

Fliesler SJ, Anderson RE. Chemistry and metabolism of lipids in the vertebrate retina. Progress in Lipid Research. 1983; 22:79–131. [PubMed: 6348799]

Fliesler SJ, Bretillon L. The ins and outs of cholesterol in the vertebrate retina. Journal of Lipid Research. 2010; 51:3399–3413. [PubMed: 20861164]

Futterman A, Futterman S. The stability of 11-cis-retinal and reactivity toward nucleophiles. Biochimica et Biophysica Acta (BBA) – Lipids and Lipid Metabolism. 1974; 337:390–394.

Groenendijk GW, Jacobs CW, Bonting SL, Daemen FJ. Dark isomerization of retinals in the presence of phosphatidylethanolamine. European Journal of Biochemistry/FEBS. 1980; 106:119–128. [PubMed: 7341223]

Gulcan HG, Alvarez RA, Maude MB, Anderson RE. Lipids of human retina, retinal pigment epithelium, and Bruch’s membrane/choroid: comparison of macular and peripheral regions. Investigative Ophthalmology & Visual Science. 1993; 34:3187–3193. [PubMed: 8407228]

Haralampus-Grynaviski NM, Lamb LE, Clancy CM, Skumatz C, Burke JM, Sarna T, Simon JD. Spectroscopic and morphological studies of human retinal lipofuscin granules. Proceedings of the National Academy of Sciences of the United States of America. 2003; 100:3179–3184. [PubMed: 12612344]

Julien S, Schraermeyer U. Lipofuscin can be eliminated from the retinal pigment epithelium of monkeys. Neurobiology of Aging. 2012; 33:2390–2397. [PubMed: 22244091]

Jung T, Bader N, Grune T. Lipofuscin: formation, distribution, and metabolic consequences. Annals of the New York Academy of Sciences. 2007; 1119:97–111. [PubMed: 18056959]

Kaemmerer E, Schutt F, Krohne TU, Holz FG, Kopitz J. Effects of lipid peroxidation-related protein modifications on RPE lysosomal functions and POS phagocytosis. Investigative Ophthalmology & Visual Science. 2007; 48:1342–1347. [PubMed: 17325182]

Katz ML. Potential reversibility of lipofuscin accumulation. Archives of Gerontology and Geriatrics. 2002; 34:311–317. [PubMed: 14764332]

Katz ML, Eldred GE. Retinal light damage reduces autofluorescent pigment deposition in the retinal pigment epithelium. Investigative Ophthalmology & Visual Science. 1989; 30:37–43. [PubMed: 2912913]

Katz ML, Gao CL, Rice LM. Formation of lipofuscin-like fluorophores by reaction of retinal with photoreceptor outer segments and liposomes. Mechanisms of Ageing and Development. 1996; 92:159–174. [PubMed: 9080396]

Kennedy CJ, Rakoczy PE, Constable IJ. Lipofuscin of the retinal pigment epithelium: a review. Eye (Lond). 1995; 9 (Pt 6):763–771. [PubMed: 8849547]

Kennedy CJ, Rakoczy PE, Constable IJ. A simple flow cytometric technique to quantify rod outer segment phagocytosis in cultured retinal pigment epithelial cells. Current Eye Research. 1996; 15:998–1003. [PubMed: 8921222]

Krohne TU, Stratmann NK, Kopitz J, Holz FG. Effects of lipid peroxidation products on lipofuscinogenesis and autophagy in human retinal pigment epithelial cells. Experimental Eye Research. 2010; 90:465–471. [PubMed: 20059996]

Lei L, Tzekov R, Tang S, Kaushal S. Accumulation and autofluorescence of phagocytized rod outer segment material in macrophages and microglial cells. Molecular Vision. 2012; 18:103–113. [PubMed: 22275801]

Lin JH, Lavail MM. Misfolded proteins and retinal dystrophies. Advances in Experimental Medicine and Biology. 2010; 664:115–121. [PubMed: 20238009]

Maminishkis A, Chen S, Jalickee S, Banzon T, Shi G, Wang FE, Ehalt T, Hammer JA, Miller SS. Confluent monolayers of cultured human fetal retinal pigment epithelium exhibit morphology and physiology of native tissue. Investigative Ophthalmology & Visual Science. 2006; 47:3612–3624. [PubMed: 16877436]

Mazzitello KI, Arizmendi CM, Family F, Grossniklaus HE. Formation and growth of lipofuscin in the retinal pigment epithelium cells. Physical Review E, Statistical, Nonlinear, and Soft Matter Physics. 2009; 80:051908.

McDowell, JH. Preparing rod outer segment membranes, regenerating rhodopsin and determining rhodopsin concentration. In: Hargrave, PA., editor. Methods in Neuroscience. Academic Press; San Diego: 1993. p. 123-130.

McLaren MJ, Inana G, Li CY. Double fluorescent vital assay of phagocytosis by cultured retinal pigment epithelial cells. Investigative Ophthalmology & Visual Science. 1993; 34:317–326. [PubMed: 7680023]

Miceli MV, Newsome DA. Insulin stimulation of retinal outer segment uptake by cultured human retinal pigment epithelial cells determined by a flow cytometric method. Experimental Eye Research. 1994; 59:271–280. [PubMed: 7821371]

Moiseyev G, Nikolaeva O, Chen Y, Farjo K, Takahashi Y, Ma JX. Inhibition of the visual cycle by A2E through direct interaction with RPE65 and implications in Stargardt disease. Proceedings of the National Academy of Sciences of the United States of America. 2010; 107:17551–17556. [PubMed: 20876139]

Mukherjee P, Bose S, Hurd AA, Adhikary R, Schonenbrucher H, Hamir AN, Richt JA, Casey TA, Rasmussen MA, Petrich JW. Monitoring the accumulation of lipofuscin in aging murine eyes by fluorescence spectroscopy. Photochemistry and Photobiology. 2009; 85:234–238. [PubMed: 18764899]

Ng KP, Gugiu B, Renganathan K, Davies MW, Gu X, Crabb JS, Kim SR, Rozanowska MB, Bonilha VL, Rayborn ME, Salomon RG, Sparrow JR, Boulton ME, Hollyfield JG, Crabb JW. Retinal pigment epithelium lipofuscin proteomics. Molecular & Cellular Proteomics: MCP. 2008; 7:1397–1405. [PubMed: 18436525]

Noorwez SM, Ostrov DA, McDowell JH, Krebs MP, Kaushal S. A high-throughput screening method for small-molecule pharmacologic chaperones of misfolded rhodopsin. Investigative Ophthalmology & Visual Science. 2008; 49:3224–3230. [PubMed: 18378578]

Papermaster DS. Preparation of retinal rod outer segments. Methods in Enzymology. 1982; 81:48–52. [PubMed: 6212746]

Rakoczy P, Kennedy C, Thompson-Wallis D, Mann K, Constable I. Changes in retinal pigment epithelial cell autofluorescence and protein expression associated with phagocytosis of rod outer segments in vitro. Biology of the Cell/Under the Auspices of the European Cell Biology Organization. 1992; 76:49–54. [PubMed: 1294288]

Rakoczy PE, Mann K, Cavaney DM, Robertson T, Papadimitreou J, Constable IJ. Detection and possible functions of a cysteine protease involved in digestion of rod outer segments by retinal pigment epithelial cells. Investigative Ophthalmology & Visual Science. 1994; 35:4100–4108. [PubMed: 7960592]

Schmitz-Valckenberg S, Fleckenstein M, Scholl HP, Holz FG. Fundus autofluorescence and progression of age-related macular degeneration. Survey of Ophthalmology. 2009; 54:96–117. [PubMed: 19171212]

Schutt F, Bergmann M, Holz FG, Dithmar S, Volcker HE, Kopitz J. Accumulation of A2-E in mitochondrial membranes of cultured RPE cells. Graefe's archive for clinical and experimental ophthalmology = Albrecht von Graefes Archiv fur klinische und experimentelle. Ophthalmologie. 2007; 245:391–398.

Schutt F, Ueberle B, Schnolzer M, Holz FG, Kopitz J. Proteome analysis of lipofuscin in human retinal pigment epithelial cells. FEBS Letters. 2002; 528:217–221. [PubMed: 12297308]

Sheehy MR. A flow-cytometric method for quantification of neurolipofuscin and comparison with existing histological and biochemical approaches. Archives of Gerontology and Geriatrics. 2002; 34:233–248. [PubMed: 14764326]

Sparrow JR, Boulton M. RPE lipofuscin and its role in retinal pathobiology. Experimental Eye Research. 2005; 80:595–606. [PubMed: 15862166]

Sparrow JR, Hicks D, Hamel CP. The retinal pigment epithelium in health and disease. Current Molecular Medicine. 2010a; 10:802–823. [PubMed: 21091424]

Sparrow JR, Parish CA, Hashimoto M, Nakanishi K. A2E, a lipofuscin fluorophore, in human retinal pigmented epithelial cells in culture. Investigative Ophthalmology & Visual Science. 1999; 40:2988–2995. [PubMed: 10549662]

Sparrow JR, Wu Y, Nagasaki T, Yoon KD, Yamamoto K, Zhou J. Fundus autofluorescence and the bisretinoids of retina. Photochemical & Photobiological Sciences: Official Journal of the European Photochemistry Association and the European Society for Photobiology. 2010b; 9:1480–1489.

Strunnikova N, Baffi J, Gonzalez A, Silk W, Cousins SW, Csaky KG. Regulated heat shock protein 27 expression in human retinal pigment epithelium. Investigative Ophthalmology & Visual Science. 2001; 42:2130–2138. [PubMed: 11481282]

Sugano E, Tomita H, Ishiguro S, Isago H, Tamai M. Nitric oxide-induced accumulation of lipofuscin-like materials is caused by inhibition of cathepsin S. Current Eye Research. 2006; 31:607–616. [PubMed: 16877269]

Sun M, Finnemann SC, Febbraio M, Shan L, Annangudi SP, Podrez EA, Hoppe G, Darrow R, Organisciak DT, Salomon RG, Silverstein RL, Hazen SL. Light-induced oxidation of photoreceptor outer segment phospholipids generates ligands for CD36-mediated phagocytosis by retinal pigment epithelium: a potential mechanism for modulating outer segment phagocytosis under oxidant stress conditions. The Journal of Biological Chemistry. 2006; 281:4222–4230. [PubMed: 16354659]

Terman A, Gustafsson B, Brunk UT. Autophagy, organelles and ageing. The Journal of Pathology. 2007; 211:134–143. [PubMed: 17200947]

Tzekov R, Stein L, Kaushal S. Protein misfolding and retinal degeneration. Cold Spring Harbor Perspectives in Biology. 2011; 3:a007492. [PubMed: 21825021]

Wang XC, Jobin C, Allen JB, Roberts WL, Jaffe GJ. Suppression of NF-kappaB-dependent proinflammatory gene expression in human RPE cells by a proteasome inhibitor. Investigative Ophthalmology & Visual Science. 1999; 40:477–486. [PubMed: 9950608]

Warburton S, Southwick K, Hardman RM, Secrest AM, Grow RK, Xin H, Woolley AT, Burton GF, Thulin CD. Examining the proteins of functional retinal lipofuscin using proteomic analysis as a guide for understanding its origin. Molecular Vision. 2005; 11:1122–1134. [PubMed: 16379024]

Weiter JJ, Delori FC, Wing GL, Fitch KA. Retinal pigment epithelial lipofuscin and melanin and choroidal melanin in human eyes. Investigative Ophthalmology & Visual Science. 1986; 27:145–152. [PubMed: 3943941]

Wing GL, Blanchard GC, Weiter JJ. The topography and age relationship of lipofuscin concentration in the retinal pigment epithelium. Investigative Ophthalmology & Visual Science. 1978; 17:601–607. [PubMed: 669891]

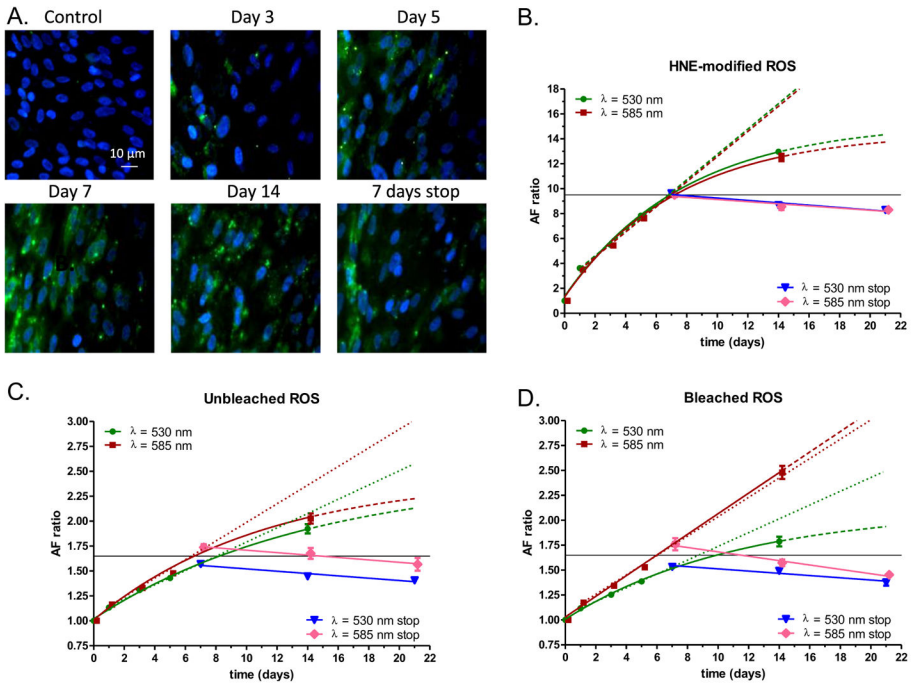

Fig. 1.

Autofluorescence of RPE cells following feeding with either bleached, unbleached, or HNE-modified ROS at different time points. **A**: Changes in RPE cells after incubation with unbleached ROS evaluated by fluorescence microscopy. Representative examples of cells in control condition (no feeding), at Day 3 and at Day 5 during incubation are presented on the top row. Representative examples of cells at Day 7 and at Day 14 during incubation and at 7 days post the end of the 14 day incubation period (7 days stop) are presented on the bottom row. The original magnification used for all micrographs was ×400. **B**–**D**: Time course of mean autofluorescence change in RPE cells (AF ratio) during and after incubation with HNE-modified ROS (**B**), unbleached ROS (**C**) or bleached ROS (**D**) detected at 533 and 585 nm. The green and red symbols indicate AF ratio from Day 1 to Day 14 at 530 nm and at 585 nm, respectively. The blue and pink symbols indicate AF ratios at 530 and 585 nm respectively, for the period Day 7 to Day 21, when no incubation took place (530 stop and 585 nm stop). Exponential curve fitting is indicated with green and red solid lines for 530 and 585 nm, respectively, and extrapolation until Day 21 is presented with dashed lines. A linear regression model (Day 1 to Day 7) is indicated with the same colors and solid lines, while the extrapolation until Day 21 is indicated with dotted lines. Similarly, a linear regression model is presented with sold blue and pink lines for 530 and 585 nm. Symbols represent average values of relative autofluorescence (AF ratio) ±SEM, whereas horizontal thin solid line indicates the level of autofluorescence at Day 7. For more details see the main text.

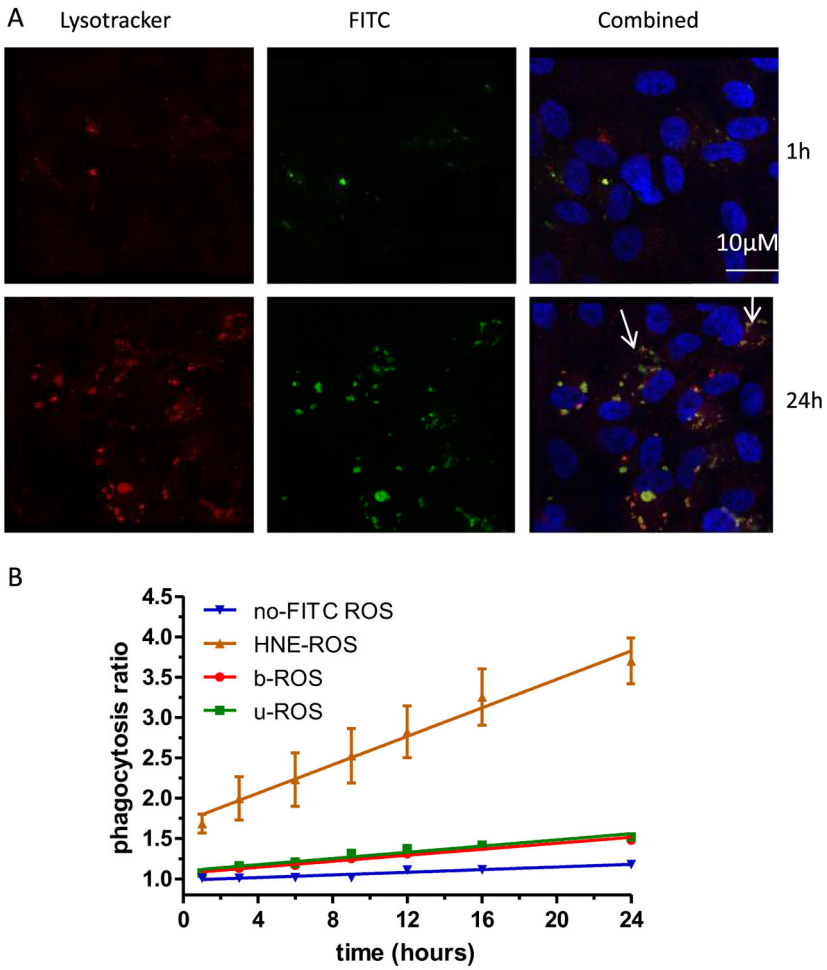

Fig. 2.

Kinetics of ROS phagocytosis by RPE cells in vitro. **A**: Confocal micrographs of ARPE-19 cells stained with either the fluorescent acidotropic probe Lysotracker Red (left panels) or with FITC-modified HNE-ROS (central panels). The right panels represent a combination of the two stains. Micrographs taken at 24 h (bottom row) demonstrate the presence of more lysosomes co-localized with FITC-labeled ROS, as indicated by white arrows. **B**: Time course of autofluorescence change generated by RPE phagocytosis of FITC-labeled ROS at various time points during the 24 h period after single feeding with 4 μg/cm^2 of four different types of ROS: Uunbleached ROS labeled with FITC, bleached ROS labeled with FITC, HNE-modified ROS labeled with FITC or unbleached ROS not labeled with FITC. The symbols indicate mean values of phagocytosis (±SEM) normalized to non-fed cells. The autofluorescence was detected and quantified by FACS in the FITC channel (530 nm).

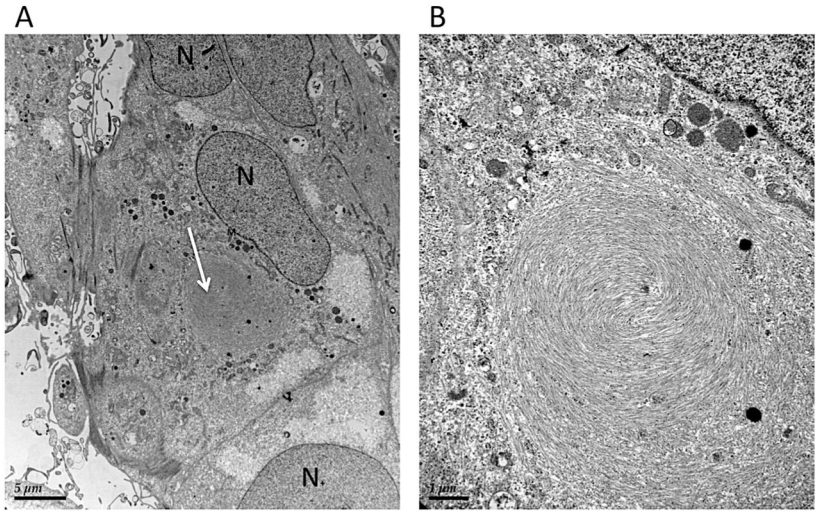

Fig. 3.

Transmissions electron microscopy of ARPE-19 cell one hour after feeding with bleached ROS. **A**: Electron micrographs of ARPE-19 cells fixed at 1 h post-feeding with bleached ROS at 4 μg/cm^2. White arrow indicates a large intracellular inclusion body. Magnification: ×2550; **B**: Higher magnification of the intracellular inclusion body presented in **A**. Magnification: ×4200. Abbreviations: N – nucleus, M – mitochondria.

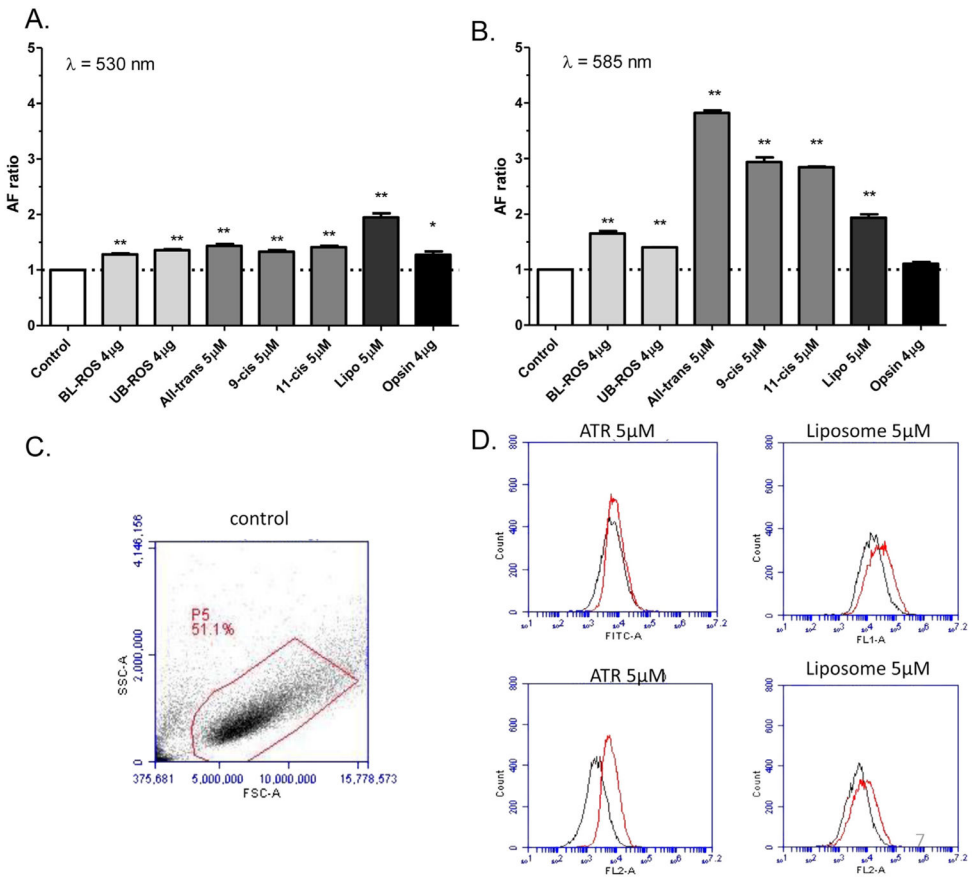

Fig. 4.

Autofluorescence of ARPE-19 cells following 7 day feeding with different preparations **A**: FACS analysis in FITC channel (detection filter wavelength, 533/30 nm) of the different groups presented in cells fed with different preparations. **B**: FACS analysis for the same conditions as in **A**, but in PE channel (detection filter wavelength, 585/40 nm); **C**: Representative example of a density plot (forward scatter vs. side scatter) from the FACS analysis under control conditions; the gate (red polygonal line) was set to exclude cell debris and cell clusters. **D**: Histograms for some of the data presented on panels **A** and **B**. Top row: histograms of control conditions (black traces) and test conditions (red traces) in the FITC channel. From left to right: all-trans-retinal condition, liposome condition. Bottom row: histograms of same conditions as in the top row, but recorded in the PE channel. Asterisks above bar graphs in **A** and **B** indicate statistical significance between the average LLAF in the control condition and the relative LLAF from cells fed with different components (one-sample *t*-test; **p* < 0.05; ***p* < 0.01).

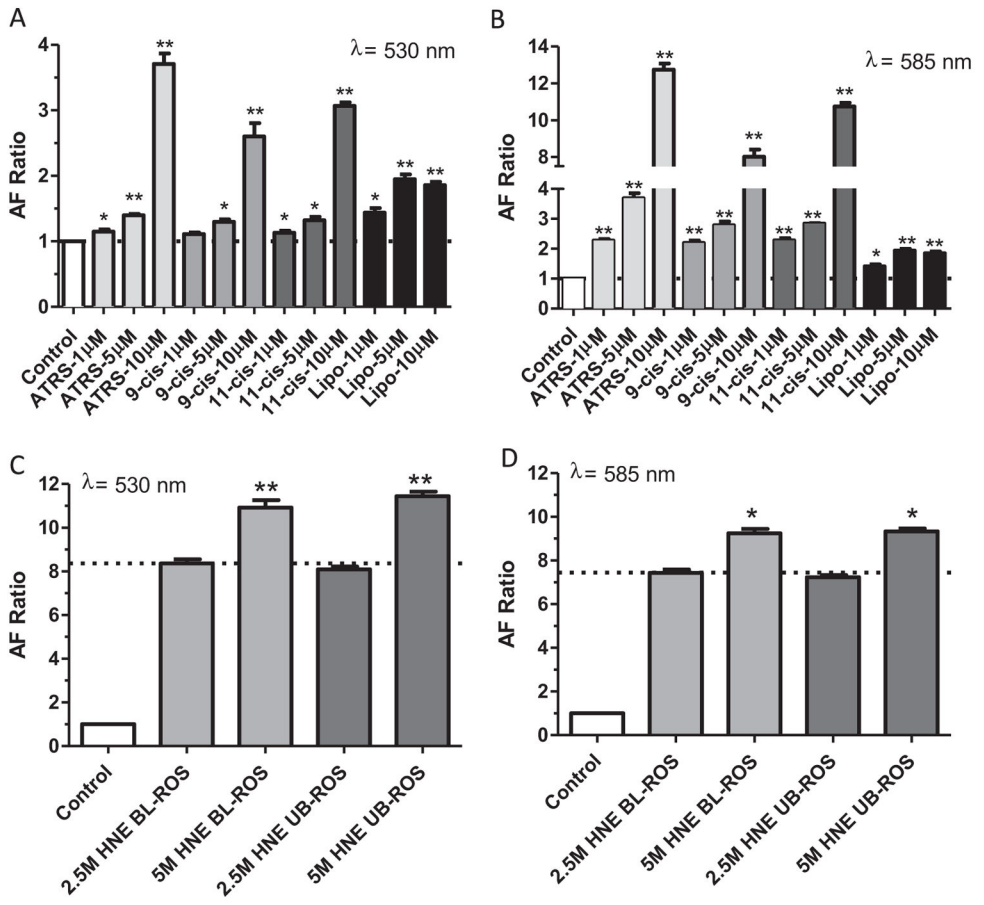

Fig. 5.

Effect of retinoids and liposomes on RPE cell autofluorescence. **A**: Average LLAF of ARPE-19 cells examined by FACS following 7 days feeding with increasing concentration of retinoids and liposomes at the FITC channel (excitation 488 nm, emission 533/30 nm). **B**: Same conditions as in **A**, but autofluorescence was detected at the PE channel (emission 585/40 nm). **C**: Average LLAF of ARPE-19 cells following 7 days feeding with different ratio of liposome and ROS. **D**: Average LLAF of ARPE-19 cells following 7 days feeding with 2 different concentrations of HNE-modified ROS (2.5 mM or 5 mM) under bleached or unbleached conditions.